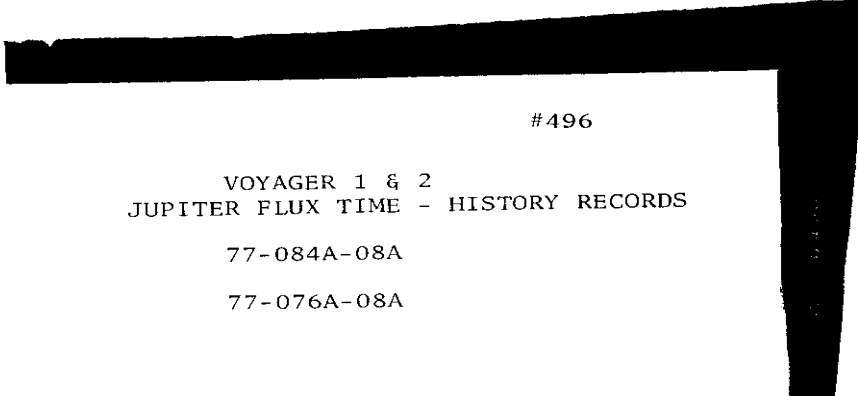


[REDACTED]

#496



VOYAGER 1 & 2  
JUPITER FLUX TIME - HISTORY RECORDS

77-084A-08A

77-076A-08A

[REDACTED]



VOYAGER 1

JUPITER FLUX TIME-HISTORY RECORDS

77-084A-08A

THIS DATA SET HAS BEEN RESTORED. ORIGINALLY IT CONTAINED ONE 9-TRACK, 1600 BPI TAPE WRITTEN IN MIXED BINARY AND EBCDIC MODE. THERE IS ONE RESTORED TAPE. THE DR TAPE IS A 3480 CARTRIDGE AND THE DS TAPE IS 9-TRACK, 6250 BPI. THE ORIGINAL TAPE WAS CREATED ON AN IBM 360 COMPUTER AND WAS RESTORED ON THE MRS SYSTEM. THE DR AND DS NUMBER ALONG WITH THE CORRESPONDING D NUMBER AND THE TIME SPAN IS AS FOLLOWS:

DR#	DS#	D#	FILES	TIME SPAN
DR004407	DS004407	D045265	9	02/28/79 - 03/16/79

VOYAGER 2  
JUPITER FLUX TIME-HISTORY RECORDS  
77-076A-08A

This data set has been restored. There was originally one 9-track, 1600 BPI tape written in Binary. There is one restored tape. The DR tape is a 3480 cartridge and the DS tape is 9-track, 6250 BPI. The original tape was created on an IBM 360 computer and the restored tape was created on an IBM 9021 computer. The DR and DS numbers along with the corresponding D numbers are as follows:

DR#	DS#	D#	FILES	TIME SPAN
-----	-----	-----	-----	-----
DR004367	DS004367	D045266	9	07/03/79 - 08/04/79

REQ. AGENT

LSM

RAND NO.

V0083

ACQ. AGENT

RWV

VOYAGER 1 & 2

JUPITER FLUX TIME - HISTORY RECORDS

77-084A-08A

77-076A-08A

This data set catalog consists of 2 tapes. The tapes are 9 track, 1600, mixed mode with 9 files of data each. The tapes were created on an IBM 360 computer.

The time spans are as follows:

VOYAGER 1

<u>D#</u>	<u>C#</u>	<u>TIME SPAN</u>
D-45265	C-21540	02/28/79 - 03/17/79

VOYAGER 2

<u>D#</u>	<u>C#</u>	<u>TIME SPAN</u>
D-45266	C-21541	07/03/79 - 08/04/79

VOYAGER 1 AND 2  
COSMIC RAY SUBSYSTEM  
**Description of Jupiter Encounter Data**

Instrumentation

As its name implies, the Cosmic Ray Subsystem (CRS) was designed for cosmic ray studies (Stone et al., 1977). It consists of two High Energy Telescopes (HET), four Low Energy Telescopes (LET) and The Electron Telescope (TET). The detectors have large geometric factors ( $\sim 0.48$  to  $8 \text{ cm}^2 \text{ ster}$ ) and long electronic time constants ( $\sim 24 \mu\text{sec}$ ) for low power consumption and good stability. Normally, the data are primarily derived from comprehensive ( $\Delta E_1$ ,  $\Delta E_2$  and  $E$ ) pulse-height information about individual events. Because of the high particle fluxes encountered at Jupiter and Saturn, greater reliance had to be placed on counting rates in single detectors and various coincidence rates. The detectors used for most of our work are listed in Table 1 and illustrated in Figure 1. In interplanetary space, guard counters are placed in anticoincidence with the primary detectors to reduce the background from high-energy particles penetrating through the sides of the telescopes. These guard counters were turned off in the Jovian magnetosphere when the accidental anticoincidence rate became high enough to block a substantial fraction of the desired counts. Fortunately, under these conditions the spectra were sufficiently soft that the background, due to penetrating particles, was small.

The data on proton and ion fluxes at Jupiter were obtained with the LET. The thicknesses of individual solid-state detectors in the LET and their trigger thresholds were chosen such that, even in the Jovian magnetosphere, electrons made, at most, a very minor contribution to the proton counting rates (Lupton and Stone, 1972). Dead time corrections and accidental

coincidences were small (< 20%) throughout most of the magnetotail, but were substantial (> 50%) at flux maxima within 40 R<sub>J</sub> of Jupiter. Data have been included in this package for those periods when the corrections are less than ~ 50% and can be corrected by the user with the dead time appropriate to the detector (2 to 25  $\mu$ sec). The high counting rates, however, caused some baseline shift which may have raised proton thresholds significantly. In the inner magnetosphere, the L<sub>2</sub> counting rate was still useful because it never rolled over. This rate is due to 1.8- to 13-MeV protons penetrating L<sub>1</sub> (0.43 cm<sup>2</sup> ster) and > 9-MeV protons penetrating the shield (8.4 cm<sup>2</sup> ster). For an E<sup>-2</sup> spectrum, the two groups would make comparable contributions; but in the magnetosphere, for the E<sup>-3</sup> to E<sup>-4</sup> spectrum above 2.5 MeV (McDonald et al., 1979), the contribution from protons penetrating the shield would be only 3 to 14%.

The LET L<sub>1</sub>L<sub>2</sub>L<sub>4</sub><sup>-</sup> and L<sub>1</sub>L<sub>2</sub>L<sub>3</sub> coincidence-anticoincidence rates give the proton flux between 1.8 and 8 MeV and 3 to 8 MeV with a small alpha particle contribution ( $\sim 10^{-3}$ ). Corrections are required for dead time losses in L<sub>1</sub>, accidental L<sub>1</sub>L<sub>2</sub> coincidences and anticoincidence losses from L<sub>4</sub>. Data are given only for periods when these corrections are relatively small. In addition to the rates listed in the table, the energy lost in detectors L<sub>1</sub>, L<sub>2</sub> and L<sub>3</sub> was measured for individual particles. For protons, this covered the energy range from 0.42 to 8.3 MeV. Protons can be identified positively by the  $\Delta E$  vs. E technique, their spectra obtained and accidental coincidences greatly reduced. Because of telemetry limitations, however, only a small fraction of the events could be transmitted, and statistics become poor unless pulse-height data are averaged over a period of one hour.

HET and LET detectors share the same data lines and pulse-height analyzers; thus, the telescopes can interfere with one another during periods

of high counting rates. To prevent such an interference and explore different coincidence conditions, the experiment was cycled through four operating modes, each 192 seconds long. Either the HETs or the LETs were turned on at a time. LET-D was cycled through L<sub>1</sub> only and L<sub>1</sub>L<sub>2</sub> coincidence requirements. The TET was cycled through various coincidence conditions, including singles from the front detectors. At the expense of some time resolution, this procedure permitted us to obtain significant data in the outer magnetosphere and excellent data during the long passage through the magnetotail region.

Some of the published results from this experiment required extensive corrections for dead time, accidental coincidences and anticoincidences (Vogt et al., 1979a, 1979b; Schardt et al., 1981; Gehrels et al., 1981). These corrections can be applied only on a case-by-case basis after a careful study of the environment and many self-consistency checks. They cannot be applied on a systematic basis and we have no computer programs to do so; therefore, data from such periods are not included in the Data Center submission. The scientists on the CRS team will, however, be glad to consider special requests if the desired information can be extracted from the data.

In order to acquaint the potential user of these data with the type of information that can be extracted from the CRS data, we are showing typical rates and fluxes in Figures 2 through 7.

#### Description of the Data

- (1) LD1 RATE gives the nominal > 0.43-MeV proton flux cm<sup>-2</sup>s<sup>-1</sup>sr<sup>-1</sup>. This rate includes all particles which pass through a 0.8 mg/cm<sup>2</sup> aluminum foil and deposits more than 220 keV in a 34.6  $\mu$  Si detector on Voyager 1 (209 keV, 33.9  $\mu$  on Voyager 2). Therefore, heavy ions, such as oxygen and sulfur are also detected; however, their contribution is believed to be relatively

small. Only a small percentage of the pulses in this detector are larger than the maximum energy that can be deposited by a proton. Heavy ions would produce such large pulses, unless their energy spectra were much steeper than the proton spectrum. The true flux,  $F_t$ , can be calculated from the data:

$$F_t = \frac{F}{1 - 1.26 \times 10^{-4} F}$$

and corrections are small for  $F < 1000 \text{ cm}^{-2}\text{s}^{-1}$ .

- (2) LD2 RATE is not suitable for an absolute flux determination and is given in counters per s. The detector responds to protons and ions that penetrate either (a)  $0.8 \text{ mg/cm}^2$  Al plus  $8.0 \text{ mg/cm}^2$  Si and lose at least 200 keV in a  $35 \mu \text{ Si}$  detector (1.8 to 13 MeV) or (b) pass through  $> 140 \text{ mg/cm}^2$  Al. For an  $E^{-2}$  proton spectrum, the contributions from (a) and (b) would be about equal; however, the proton spectrum is substantially softer throughout most of the magnetosphere and the detector should respond primarily to (a). Dead time corrections are given by

$$R_t = \frac{R}{1 - 2.55 \times 10^{-5} R}$$

where  $R$  is the count rate in counts/s. Thus, correction to the supplied data are small for  $R < 4000 \text{ c/sec}$ , but become so large in the middle magnetosphere that the magnitude of even relative intensity changes becomes uncertain.

- (3) LD  $L_1 \cdot L_2 \cdot L_4$ . SL COINCIDENCE RATE gives the total proton flux ( $\text{cm}^{-2}\text{s}^{-1}\text{sr}^{-1}$ ) between  $\sim 1.8$  and  $\sim 8.1$  MeV with a small admixture of alpha particles. Accidental coincidences become substantial at higher rates and

the flux derived from pulse-height analysis should be used if accuracy is desired.

- (4) LDTRP RATE gives proton flux ( $\text{cm}^{-2}\text{s}^{-1}\text{sr}^{-1}$ ) between 3.0 and 8.0 MeV with a small alpha particle contribution ( $L_1L_2L_3$  coincidences are required).
- (5) IBS4E RATE gives the electron flux ( $\text{cm}^{-2}\text{s}^{-1}\text{sr}^{-1}$ ) for electrons with a range between 4 and 10 mm in Si; this corresponds approximately to the energy range of 2.6-5.1 MeV. Accidental coincidence and dead time corrections are generally small in the magnetotail and have not been applied to these data. Because of differences between Voyager 1 and 2, we give the average rate for HET I and II for Voyager 1 and the HET I rate for Voyager 2.
- (6) IBS3E RATE is the same as (5); but the electron range falls between 10 and 16 mm of Si, or approximately 5.1-8 MeV.
- (7) IBS2E RATE is the same as (5); but the electron range falls etween 16 and 22 mm of Si, or approximately 8-12 MeV.
- (8) D4L RATE is not suitable for an absolute electron flux determination. This counting rate includes all pulses from detector D<sub>4</sub> of TET (Fig. 1) which exceed 0.5 MeV. The shielding varies with direction of incidence but is at least 1.2 cm of Si. In the Jovian environment, the detector responds primarily to electrons with energies above  $\sim 6$  MeV. The D<sub>4L</sub> rate is useful primarily for determining relative changes in the high-energy electron flux. This rate has a high background from the RTG. Where needed, the dead time corrections should be applied as to the LD<sub>2</sub> rate ( $\tau \sim 2.55 \times 10^{-5} \text{ s}$ ).
- (9) Pulse-height Analyzed Proton Flux (FPHA) is derived from a  $\Delta E$  vs. E analysis of pulses from L<sub>1</sub>, L<sub>2</sub> and L<sub>3</sub> of LET (Fig 1) and gives the

average proton flux ( $\text{cm}^{-2}\text{s}^{-1}\text{sr}^{-1}\text{MeV}^{-1}$ ) in six energy channels. Where required, a correction should be applied for the dead time in LD1 as follows:

$$\text{FPHA}_t = \frac{\text{FPHA}}{1 - 1.26 \times 10^{-4} \text{FLD1}}$$

where FPHA is the listed flux of this rate (9) and FLD1 is the flux given in rate 1. FPHA gives the most accurate value of the proton flux available from this experiment; however, the counting statistics are poorer than for the other rates because of limited sampling. Fluxes derived from rate 3 (LD) which cover the same energy range as FPHA will be higher because of poorer definition of the energy threshold, accidental coincidences and a variable, but small, background contribution.

#### ENERGY CHANNELS (MEV) OF FPHA

(absolute accuracy  $\sim 10\%$ )

#### VOYAGER 1

1	1.829 - 2.045
2	2.045 - 3.104
3	3.104 - 3.753
4	3.753 - 4.530
5	4.530 - 6.284
6	6.284 - 8.091

#### VOYAGER 2

1	1.807 - 2.001
2	2.001 - 3.309
3	3.309 - 3.984
4	3.984 - 4.761
5	4.761 - 6.041
6	6.041 - 8.043

Data Format

Time-history of CRS data described above is being submitted on 9-track tapes recorded at ~~1600~~<sup>1630</sup> BPI. Tape marked CRSJU1 contains Voyager 1 data and the one marked CRSJU2 contains Voyager 2 data.

Each tape contains nine files. Contents of CRSJU1 are described in Table 2, and those of CRSJU2 appear in Table 3. Each file consists of a number of Flux Time-History (FTH) records. An FTH record contains a count of the number of data items (NBIN) whose time-history is included in the record, a count of the number of averaging intervals (NINT) included in the record, definitions of data items included and time-history data. Table 4 defines the structure of an FTH record in detail. These tapes were generated on an IBM System 360 computer; thus, a word consists of 32 bits, half-word 1 is the high order 16-bit field of the word and half-word 2 the low order half (bits 16-31, with the left-most or MSB numbered 0). Characters are represented in 8-bit EBCDIC byte, real numbers are represented in the IBM single precision floating point format. Length (in words) of an FTH record is given by

$$200 + (3 + 2 * \text{NBIN}) * \text{NINT} \quad \text{NBIN} \leq 5$$

$$233 + (3 + 2 * 6) * \text{NINT} \quad \text{NBIN} = 6$$

For all files on CRSJU1 and CRSJU2, NINT  $\leq$  96. For file 9, NINT  $\leq$  24. Thus, maximum record length is 680 words (2720 bytes) for files 1-4 and 8, 872 words (3488 bytes) for files 5-7 and 593 words (2372 bytes) for file 9.

Table 1  
CRS DETECTORS USED DURING JUPITER ENCOUNTER

Detector	Shielding	Energy Range <sup>+</sup> (MeV)	Factor (cm <sup>2</sup> ster)	Comments
PROTONS (LET):				
L1*	0.8 mg/cm <sup>2</sup> Al	0.42-12	4.5	Also, alphas above 0.32 MeV/n
L2*	8.1 mg/cm <sup>2</sup> Si	1.8 -13	0.43	Through L1
	>140 mg/cm <sup>2</sup> Al	>9	8.4	Protons through side. The intensity is comparable to those through front for E <sup>-2</sup> spectrum
L1 L2 T4	1.8 - 8		0.43	ΔE - E analysis
ELECTRONS (HET):				
Range:	4-10 mm Si	2.6- 5.1	1.46	Coincidence rates with good background rejections, but accidental coincidence problems at high counting rates (for details, see Stone et al., 1977).
	10-16 mm Si	5.8- 8	1.25	
	16-22 mm Si	8 -12	0.96	
ELECTRONS (TET):				
D4 (3 mm Si) .	~1.2 cm Si equivalent	>6	~14	Usable at higher flux than HET rates

\*Single rates

<sup>+</sup>Small difference between similar detectors

Table 2. CONTENTS OF CRSJU1

FILE #	DATA ITEM	AVERAGING INTERVAL	TIME PERIOD
1	LD1 RATE	15 min.	2/28/79, 00:00, to 3/04/79, 12:00 3/06/79, 06:45, to 3/17/79, 00:00
2	LD2 RATE	15 min.	2/28/79, 00:00, to 3/09/79, 12:00
3	LD RATE	15 min.	2/28/79, 00:00, to 3/03/79, 12:00 3/07/79, 08:00, to 3/17/79, 00:00
4	LDTRP RATE	15 min.	Same as for LD RATE
*	BS4E RATE	15 min.	2/28/79, 00:00, to 3/03/79, 00:00 3/07/79, 08:00, to 3/17/79, 00:00
*	BS3E RATE	15 min.	Same as for BS4E RATE
*	BS2E RATE	15 min.	Same as for BS4E RATE
8	D4L RATE	15 min.	2/28/79, 00:00, to 3/04/79, 20:00 3/06/79, 02:00, to 3/08/79, 00:00
9	FPHA	1 hour	2/28/79, 00:00, to 3/03/79, 12:00 3/07/79, 08:00, to 3/17/79, 00:00

---

\*These files nominally contain two quantities, the rate when guard anticoincidence is required and the rate when guard term is deleted from coincidence requirement. The experiment is in the latter state from ~ 01:15:00, March 2, 1979, to ~ 20:15:00, March 2, 1979. Note also that HET-I and HET-II data are averaged in these files.

Table 3. CONTENTS OF CRSJU2

FILE #	DATA ITEM	AVERAGING INTERVAL	TIME PERIOD
1	LD1 RATE	15 min.	7/03/79, 00:00, to 7/08/79, 12:00 7/11/79, 12:00, to 8/04/79, 00:00
2	LD2 RATE	15 min.	7/03/79, 00:00, to 7/14/79, 00:00
3	LD RATE	15 min.	7/03/79, 00:00, to 7/06/79, 00:00 7/11/79, 18:00, to 8/04/79, 00:00
4	LDTRP RATE	15 min.	Same as LD RATE
*	BS4E RATE	15 min.	7/03/79, 00:00, to 7/06/79, 04:00 7/12/79, 12:00, to 8/04/79, 00:00
*	BS3E RATE	15 min.	Same as BS4E RATE
*	BS2E RATE	15 min.	Same as BS4E RATE
8	D4L RATE	15 min.	7/03/79, 00:00, to 7/08/79, 12:00 7/11/79, 12:00, to 8/14/79, 00:00
9	FPHA	1 hour	7/03/79, 00:00, to 7/06/79, 04:00 7/11/79, 18:00, to 8/04/79, 00:00

---

\*These files nominally contain two quantities, the rate when guard anticoincidence is required and the rate when guard term is deleted from coincidence requirement. The experiment is in the latter state from ~ 12:15:00, July 12, 1979, to ~ 06:15:00, July 18, 1979.

Table 4. STRUCTURE OF FLUX TIME-HISTORY RECORD

WORD	HALFWORD	TYPE	DESCRIPTION
1	1	Integer	Number of data items contained in the record (NBIN).
.	2	Integer	Number of averaging intervals (NINT) contained in the record.
3-35		character	132-character title identifies satellite and gives the start time of first averaging interval and last averaging interval in the record.
36-68		character	132-character description of first data item.
69-101		character	132-character description of second data item, if NBIN $\geq$ 2. Otherwise, not used.
102-134		character	132-character description of third data item, if NBIN $\geq$ 3. Otherwise, not used.
135-167		character	132-character description of fourth data item, if NBIN $\geq$ 4. Otherwise, not used.
168-200		character	132-character description of fifth data item, if NBIN $\geq$ 5. Otherwise, not used.
<u>NBIN <math>\leq</math> 5</u>			
201-			NINT Averaging Interval Entries (AIE). The structure of an AIE is shown in Table 5.
NBIN = 6			
201-233		character	132-character description of sixth data item.
234-			NINT Averaging Interval Entries.

Table 5. STRUCTURE OF AVERAGING INTERVAL ENTRY

WORD	HALFWORD	TYPE	DESCRIPTION	
1	1	Integer	2-digit year	month of year
	2	Integer	month of year	
2	1	Integer	day of month	Start time of averaging interval
	2	Integer	hour of day	
3	1	Integer	minute of hour	second of minute
	2	Integer	second of minute	
4- (3+2*NBIN)		Real	NBIN FLUX entries. Each FLUX entry is two words long. If the second word of the entry is -1.0, data for this item is not available; otherwise the first word is the value of flux and the second word contains the associated statistical error.	

## REFERENCES

- Gehrels, N., E.C. Stone and J.H. Trainor, "Energetic Oxygen and Sulfur in the Jovian Magnetosphere," submitted to J. Geophys. Res., 1981.
- Lupton, J.E., and E.C. Stone, "Measurement of Electron Detection Efficiencies in Solid-state Detectors," Nucl. Instr. and Meth. 98, 189, 1972.
- McDonald, F.B., A.W. Schardt and J.H. Trainor, "Energetic Protons in the Jovian Magnetosphere," J. Geophys. Res. 84, 2579, 1979.
- Schardt, A.W., F.B. McDonald and J.H. Trainor, "Energetic Particles in the Pre-dawn Magnetotail of Jupiter," J. Geophys. Res., special Voyager issue, 1981.
- Stone, E.C., R.E. Vogt, F.B. McDonald, B.J. Teegarden, J.H. Trainor, J.R. Jokipii and W.R. Webber, "Cosmic Ray Investigation for the Voyager Mission: Energetic Particle Studies in the outer Heliosphere--and Beyond," Space Sci. Rev. 21, 355, 1977.
- Vogt, R.E., W.R. Cook, A.C. Cummings, T.L. Garrard, N. Gehrels, E.C. Stone, J.H. Trainor, A.W. Schardt, T. Conlon, N. Lal and F.B. McDonald, "Voyager 1: Energetic Ions and Electrons in the Jovian Magnetosphere," Science 204, 1003, 1979a.
- Vogt, R.E., A.C. Cummings, N. Gehrels, E.C. Stone, J.H. Trainor, A.W. Schardt, T.F. Conlon and F.B. McDonald, "Voyager 2: Energetic Ions and Electrons in the Jovian Magnetosphere," Science 206, 984, 1979b.

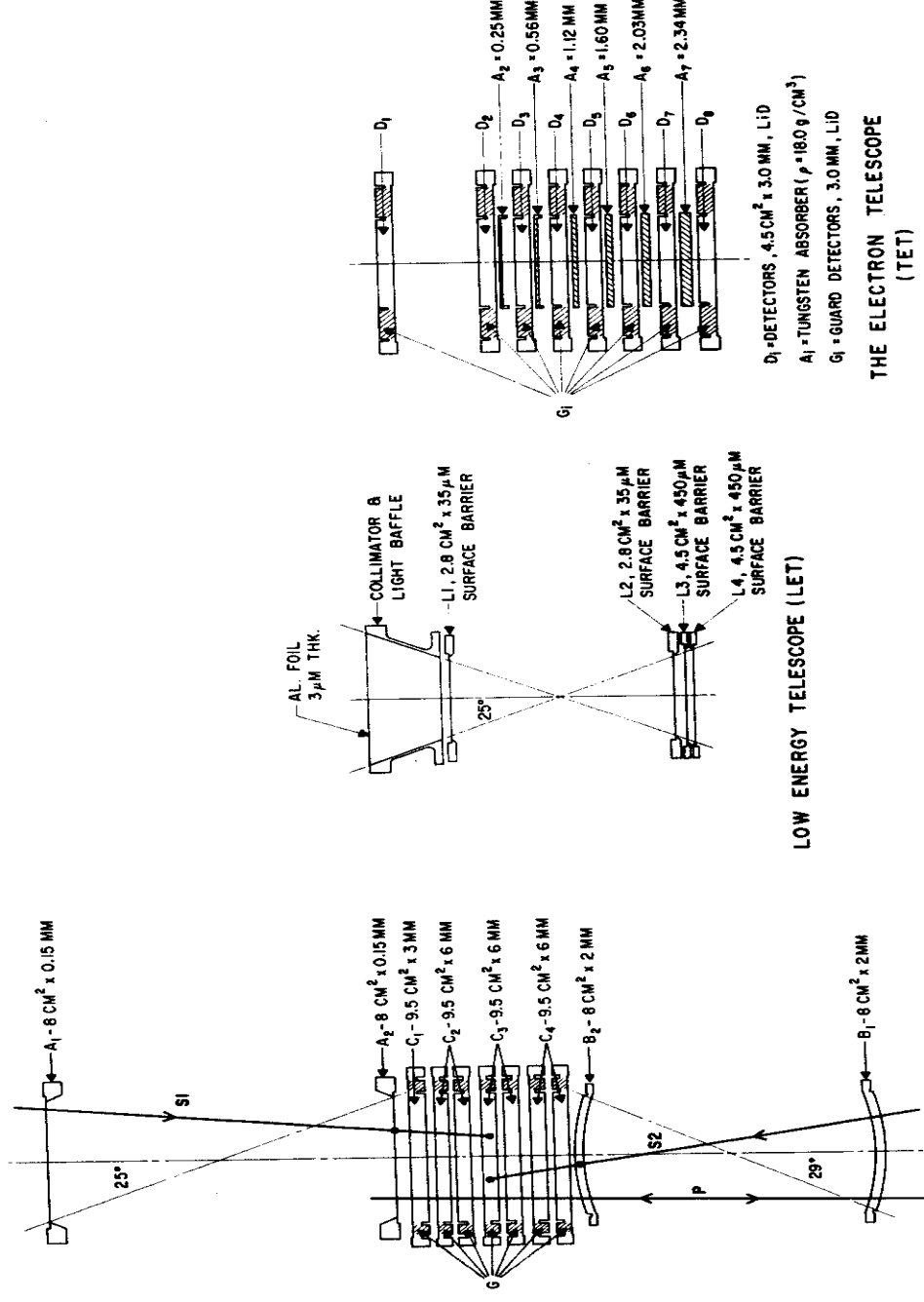


Fig. 1. Schematic diagram of the High Energy Telescope (HET), Low Energy Telescope (LET) and the Electron Telescope (TET) systems.

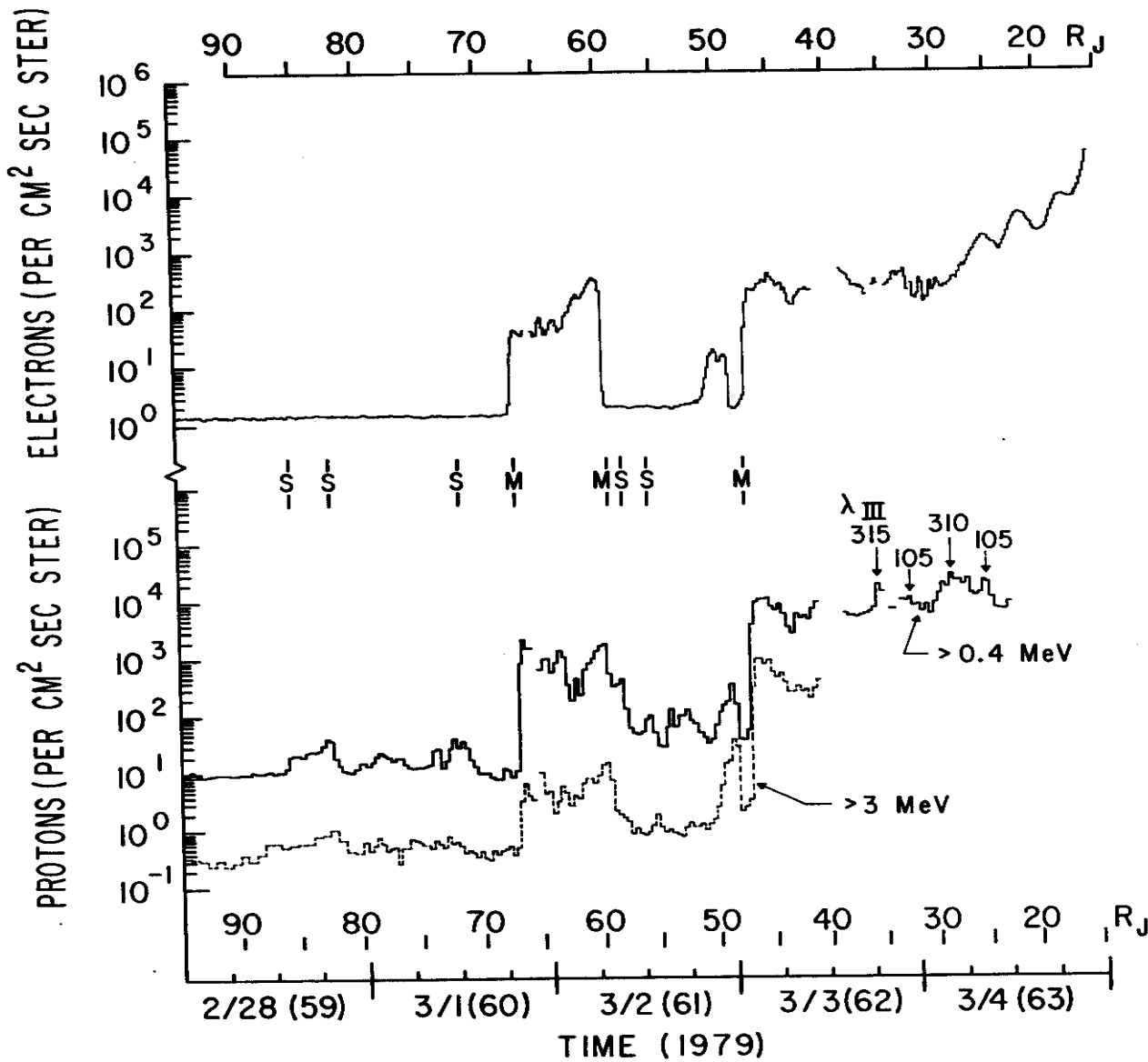


Fig. 2. Proton and  $> 5$  MeV electron flux observed during the inbound pass of Voyager 1. Bow shock and magnetopause crossings are indicated by S and M, respectively. Jovicentric longitudes ( $\lambda_{III}$  1965) of flux maxima near magnetic equatorial crossings are indicated.

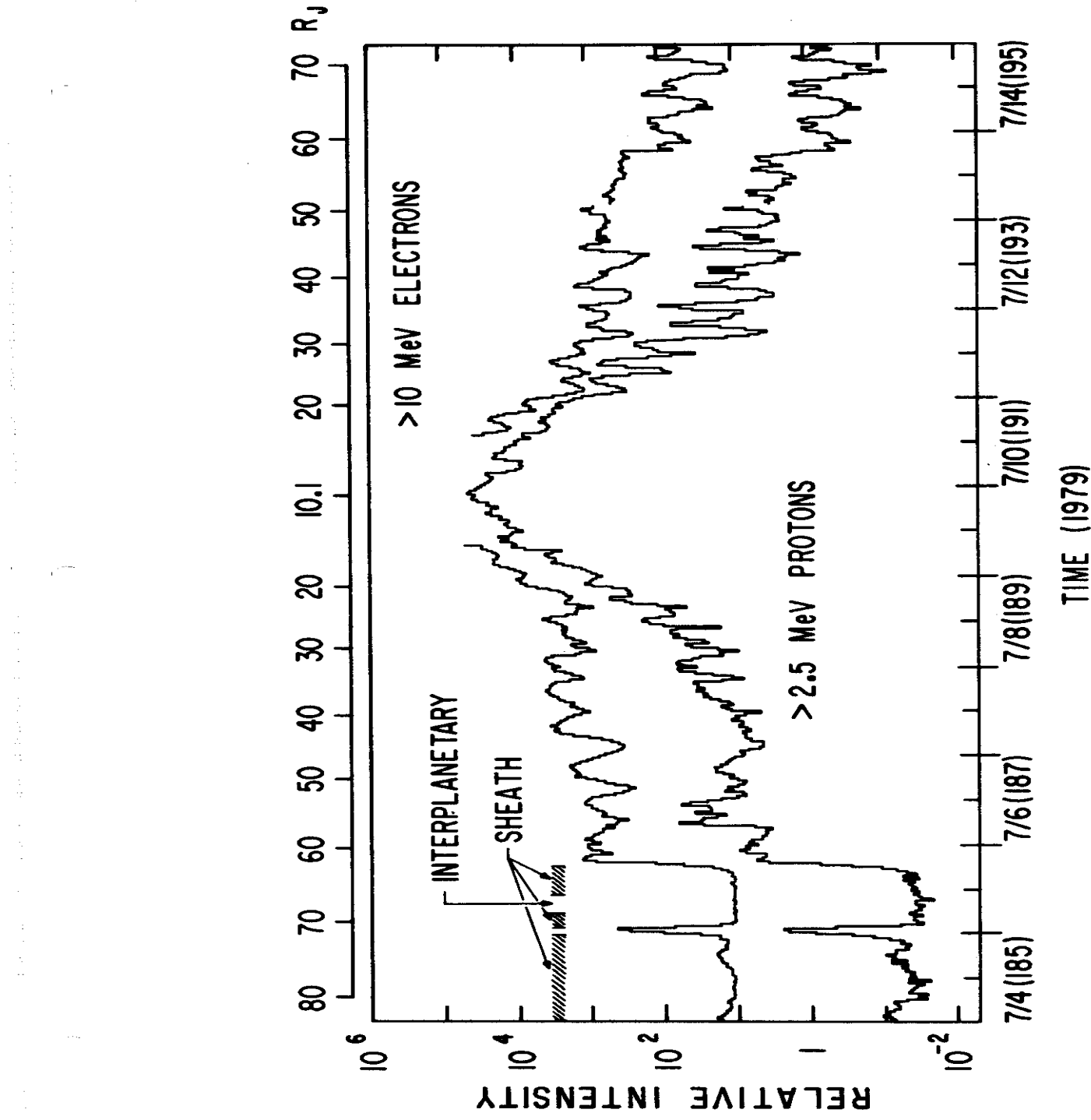


Fig. 3. Proton and electron intensities observed by Voyager 2

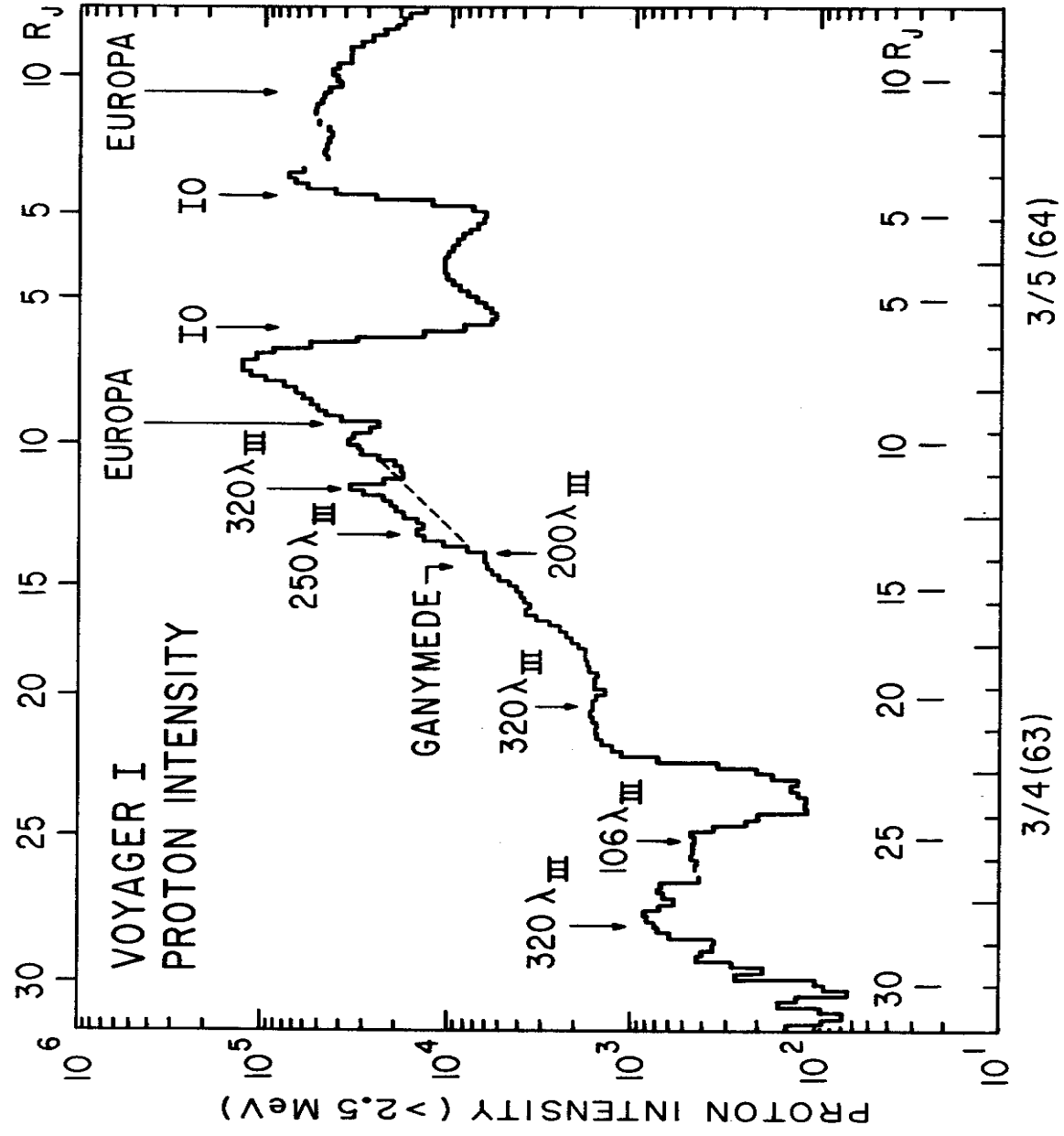


Fig. 4. Relative proton intensities in the middle magnetosphere observed with Voyager 1. Due to the extreme fluxes, the detector threshold shifted with counting rate.

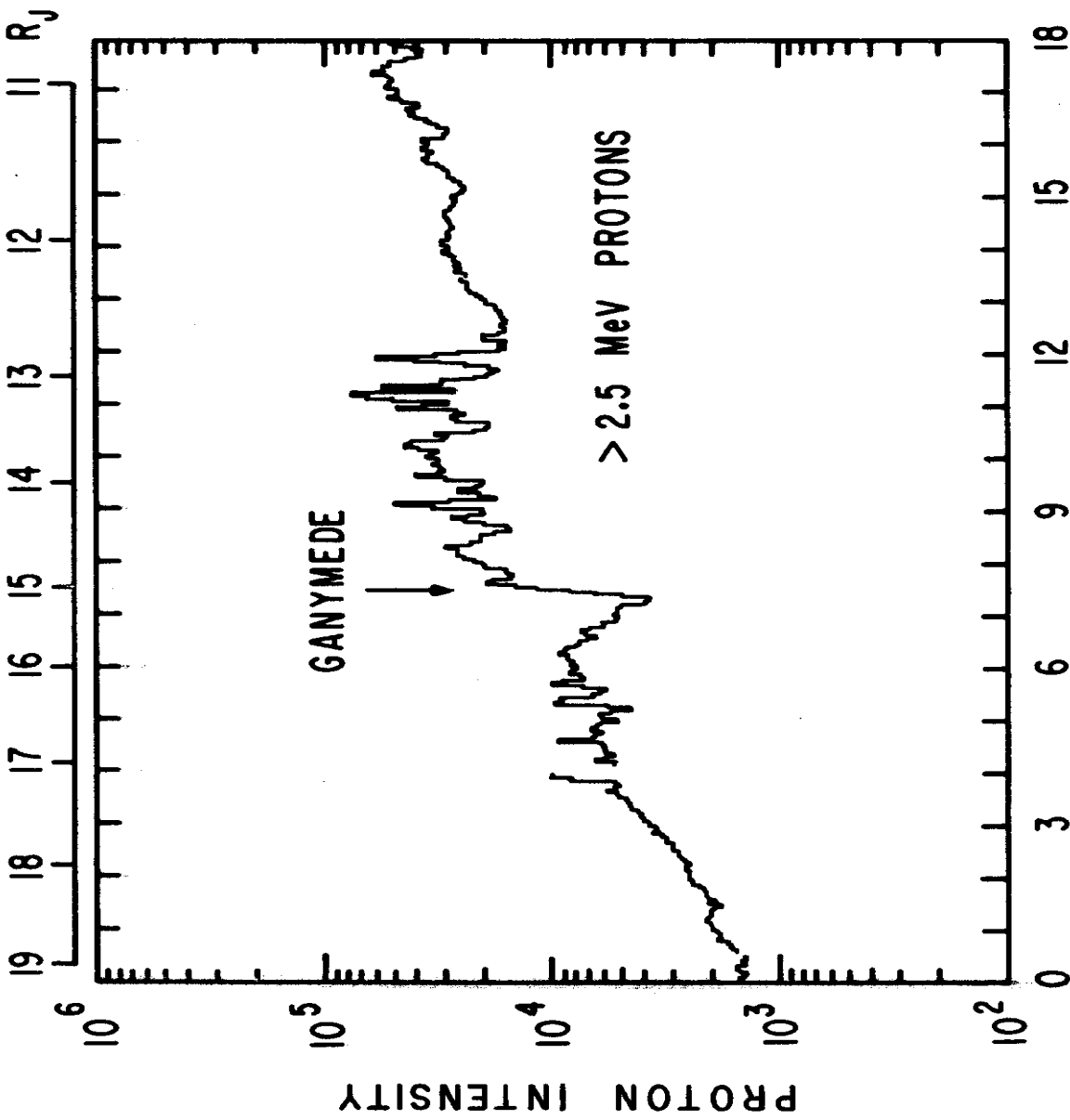


Fig. 5. Approximate intensity of protons with energies above 2.5 MeV observed with Voyager 2 near the orbit of Ganymede. Note the large intensity fluctuations which fall within  $\pm 4$  hours of the closest approach to Ganymede.

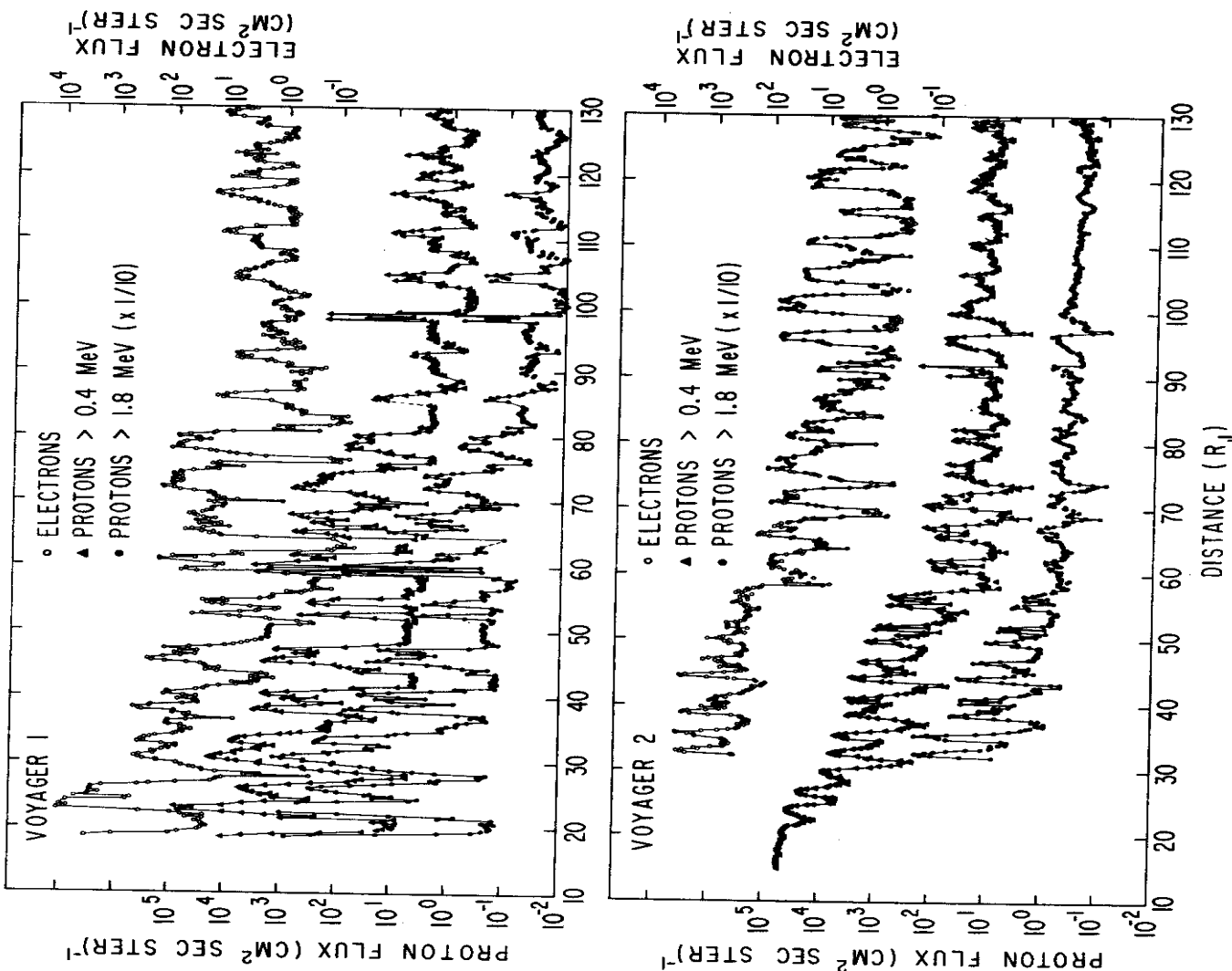


Fig. 6. Electron (2.6-5.1 MeV) and proton fluxes observed during the outbound passes of Voyagers 1 and 2. Electron and > 1.8 MeV proton fluxes above  $10^3 \text{ cm}^{-2} \text{ s}^{-1} \text{ sr}^{-1}$  are uncertain because of large corrections and show only relative trends.

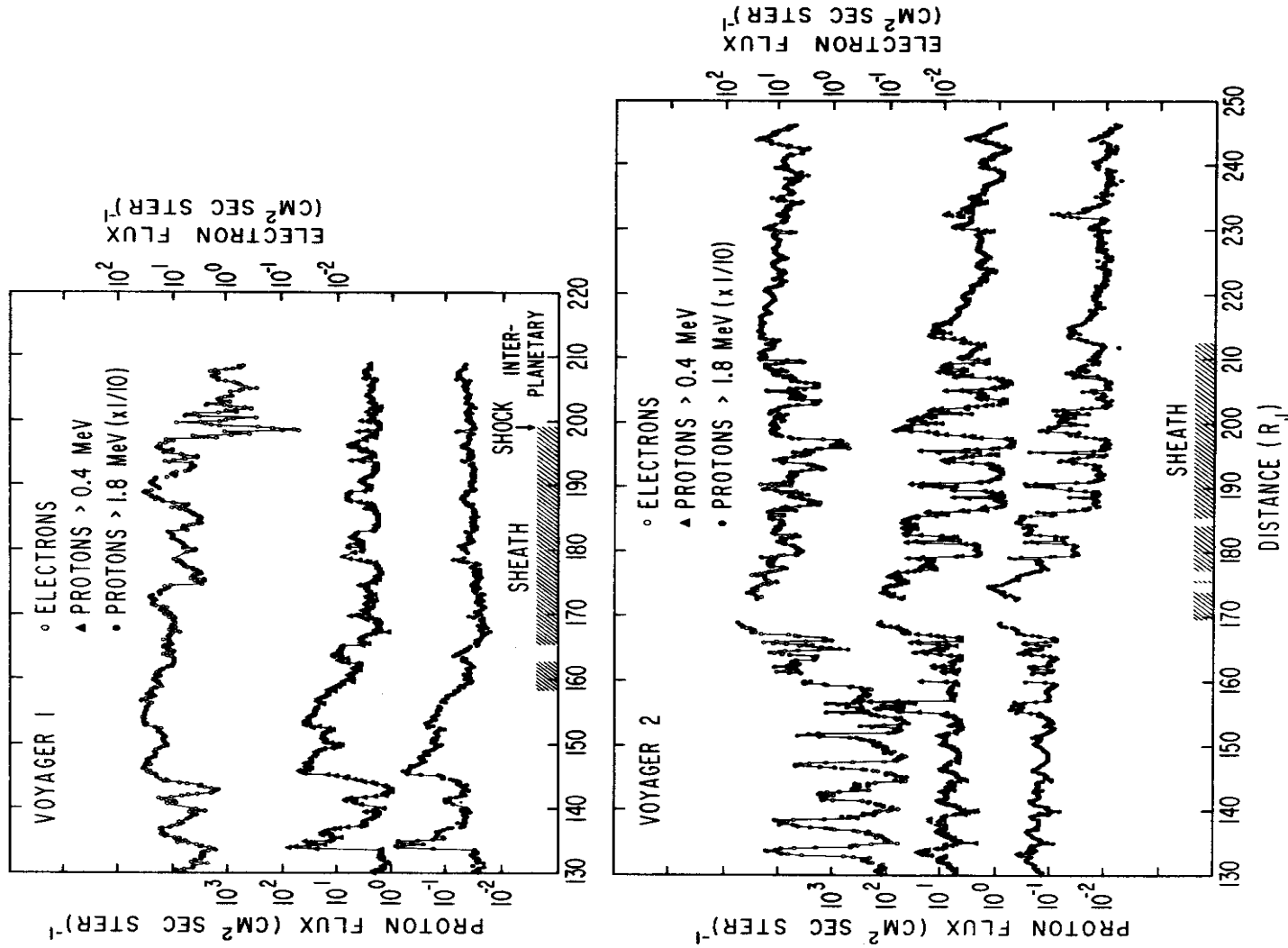


Fig. 7. The fluxes shown in Fig. 6 are extended from 130 to 250 Jovian radii. The shading near the distance scale indicates when the spacecraft were in the magnetotail.

## HEX DUMP OF cm1132

Voyage 2

DRAFT 367

FILE 1

RECORD 1 2720 BYTES

{	0)	00010060	77777777	E5D6E8C1	0705D960	F2404040	40C6D3E4	D940E3C8	C540D7C5	D9C9D6C4	
{	40)	4040F761	77777777	E5D6E8C1	7A40F07A	40F04040	D64040F7	D4140F361	F37AF4F5	7A40F040	
{	80)	40404040	40404040	40404040	40404040	40404040	40404040	40404040	40404040	40404040	
{	120)	40404040	40404040	40404040	40404040	40404040	40404040	C1407E40	40D3C4F1	604DE45D	
{	160)	C540F0F0	5D404040	40404040	40404040	40404040	40404040	40404040	40404040	40404040	
{	200)	D3C4F140	7E40D3F1	40404040	40404040	40404040	40404040	40404040	40404040	40404040	
{	240)	40404040	40404040	40404040	40404040	40404040	40404040	40404040	40404040	40404040	
{	280)	77777777	77777777	77777777	77777777	77777777	77777777	77777777	77777777	77777777	
{	320)	77777777	77777777	77777777	77777777	77777777	77777777	77777777	77777777	77777777	
{	360)	77777777	77777777	77777777	77777777	77777777	77777777	77777777	77777777	77777777	
{	400)	77777777	77777777	77777777	77777777	77777777	77777777	77777777	77777777	77777777	
{	440)	77777777	77777777	77777777	77777777	77777777	77777777	77777777	77777777	77777777	
{	480)	77777777	77777777	77777777	77777777	77777777	77777777	77777777	77777777	77777777	
{	520)	77777777	77777777	77777777	77777777	77777777	77777777	77777777	77777777	77777777	
{	560)	77777777	77777777	77777777	77777777	77777777	77777777	77777777	77777777	77777777	
{	600)	77777777	77777777	77777777	77777777	77777777	77777777	77777777	77777777	77777777	
{	640)	77777777	77777777	77777777	77777777	77777777	77777777	77777777	77777777	77777777	
{	680)	77777777	77777777	77777777	77777777	77777777	77777777	77777777	77777777	77777777	
{	720)	77777777	77777777	77777777	77777777	77777777	77777777	77777777	77777777	77777777	
{	760)	77777777	77777777	77777777	77777777	77777777	77777777	77777777	77777777	77777777	
{	800)	004F0007	00030000	00000000	412A5EAA	4027CF02	004F0007	00030000	000F0000	41318EDB	4026B20D
{	840)	004F0007	00030000	001E0000	412E5087	40299EDC	004F0007	00030000	002D0000	412D59AC	4024D644
{	880)	004F0007	00030001	00000000	412D54F	4029178E	004F0007	00030001	000F0000	412FC68D	402A459D
{	920)	004F0007	00030001	001E0000	41313517	40265F1D	004F0007	00030001	002D0000	412D3BC0	4024CA1B
{	960)	004F0007	00030002	00000000	412DE052	403A94C8	004F0007	00030002	000F0000	412A2CCB	40205DC6
{	1000)	004F0007	00030002	001E0000	412E84E4	40254F05	004F0007	00030002	002D0000	412B89E2	403911B3
{	1040)	004F0007	00030003	00000000	4130CC5D	402AB8D4	004F0007	00030003	000F0000	4130818F	402618DD
{	1080)	004F0007	00030004	00000000	4130818F	402618DD	004F0007	00030003	002D0000	412F30F0	402A0339
{	1120)	004F0007	00030004	001E0000	412CD81	4028F575	004F0007	00030004	002D0000	412E84E4	40254F05
{	1160)	004F0007	00030004	001E0000	412E8548	402DE6DA	004F0007	00030004	002D0000	413A52FE	4029C673
{	1200)	004F0007	00030005	00000000	413B0685	402EFG6D	004F0007	00030005	000F0000	41350908	40289C0
{	1240)	004F0007	00030005	001E0000	41374907	4028AC1C	004F0007	00030005	002D0000	41385653	40290EB3
{	1280)	004F0007	00030006	00000000	412E75EE	403AF3FD	004F0007	00030006	000F0000	4130F000	4022F3B0
{	1320)	004F0007	00030006	001E0000	412F9230	4025BA67	004F0007	00030006	002D0000	412F8836	4030AFD7
{	1360)	004F0007	00030007	00000000	412FB7BE	402A2478	004F0007	00030007	000F0000	412F5658	4025A2A5
{	1400)	004F0007	00030007	001E0000	412E8EDD	40302F79	004F0007	00030007	002D0000	4130CC5D	402AB8D4
{	1440)	004F0007	00030008	00000000	412BD4B0	40287D3A	004F0007	00030008	000F0000	412BD4B0	402436F1
{	1480)	004F0007	00030008	00000000	4129C90E	4027887B	004F0007	00030008	002D0000	412FCE07	4025D21B
{	1520)	004F0007	00030009	00000000	412C1F7E	40289FB8	004F0007	00030009	000F0000	412CD81	4028F575
{	1560)	004F0007	00030009	001E0000	412F1A7F	40258AD3	004F0007	00030009	002D0000	412F5658	4025A2A5
{	1600)	004F0007	0003000A	00000000	413322CD	403DD924	004F0007	0003000A	000F0000	412C068E	402121F5
{	1640)	004F0007	0003000A	001E0000	412C8838	402480D0	004F0007	0003000A	002D0000	4131172B	402436F1
{	1680)	004F0007	0003000B	00000000	412C6A4C	402F1042	004F0007	0003000B	000F0000	412FCE07	4025D21B
{	1720)	004F0007	0003000B	001E0000	41267CA	402B6B78	004F0007	0003000B	002D0000	412CD81	4028F575
{	1760)	004F0007	0003000C	00000000	41489CE	40341D3E	004F0007	0003000C	002D0000	4130BD67	40263056
{	1800)	004F0007	0003000C	001E0000	4135E972	402CE798	004F0007	0003000C	002D0000	413EC405	402B562E
{	1840)	004F0007	0003000D	00000000	41321CFC	402B4E33	004F0007	0003000D	000F0000	412FA125	402A350E
{	1880)	004F0007	0003000D	001E0000	412F9230	4025EA67	004F0007	0003000D	000F0000	412B88C	4023ADF4
{	1920)	004F0007	0003000E	00000000	412A13DC	40381A7B	004F0007	0003000E	000F0000	412D6E50	403FF9EE
{	1960)	004F0007	0003000E	001E0000	412A5EAA	4027CF02	004F0007	0003000E	002D0000	4130BD67	40263056
{	2000)	004F0007	0003000F	00000000	41243F4	4024D030	004F0007	0003000F	000F0000	4129E1FD	402DB3BD
{	2040)	004F0007	0003000F	001E0000	412B98D8	40241E2F	004F0007	0003000F	002D0000	41339302	402BEB9B
{	2080)	004F0007	00030010	00000000	41334834	402BCBBS	004F0007	00030010	000F0000	4131ACC7	40268DAB
{	2120)	004F0007	00030010	001E0000	412C44E5	4028E0EC	004F0007	00030010	002D0000	412B89E2	40285A9E
{	2160)	004F0007	00030011	00000000	412F5658	402A13DC	004F0007	00030011	000F0000	412B3F14	402837E5

FILE 1		HEX DUMP OF cn1132	
RECORD	30	1760 BYTES	
(	0)	00010030	77777777 E5D6E8C1 C705D960 F2404040
((	40)	4040F861	40F361F7 F940F1F2 7A40F07A 40F04040
((	80)	40404040	40404040 40404040 40404040 40404040
((	120)	40404040	40404040 40404040 40404040 40404040
((	160)	C540F0F0	5D404040 7E40D3F1 40404040 40404040
((	200)	D3C4F140	40404040 40404040 40404040 40404040
((	240)	40404040	40404040 40404040 40404040 40404040
((	280)	77777777	77777777 77777777 77777777 77777777
((	320)	77777777	77777777 77777777 77777777 77777777
((	360)	77777777	77777777 77777777 77777777 77777777
((	400)	77777777	77777777 77777777 77777777 77777777
((	440)	77777777	77777777 77777777 77777777 77777777
((	480)	77777777	77777777 77777777 77777777 77777777
((	520)	77777777	77777777 77777777 77777777 77777777
((	560)	77777777	77777777 77777777 77777777 77777777
((	600)	77777777	77777777 77777777 77777777 77777777
((	640)	77777777	77777777 77777777 77777777 77777777
((	680)	77777777	77777777 77777777 77777777 77777777
((	720)	77777777	77777777 77777777 77777777 77777777
((	760)	77777777	77777777 77777777 77777777 77777777
((	800)	004F0008	003000C 001E0000 41114C6E 4016C03C
((	840)	004F0008	003000C 001E0000 411998E1 401BACD7
((	880)	004F0008	003000D 0000000 4125C0C0 40219C2E
((	920)	004F0008	003000D 001E0000 4129E1FD 402050F7
((	960)	004F0008	003000E 0000000 41833340 40460D21
((	1000)	004F0008	003000E 001E0000 417689B7 40365DD9
((	1040)	004F0008	003000F 0000000 4175EF21 403B675C
((	1080)	004F0008	003000F 001E0000 419E6014 406CD846
((	1120)	004F0008	0030010 0000000 41B02432 40489916
((	1160)	004F0008	0030010 001E0000 421418AF 40621662
((	1200)	004F0008	0030011 0000000 417C93AF 4037EBF8





FILE INPUT CAPTURE ADDRESS TO SERVER  
INPUT SENDER FROM SERVER  
RECEIVE LOGIC UNIT SERVER UPDATE STATUS TABLE

THE PRACTICE  
OF MEDICINE.

Reichs-Zucker-Unternehmung

FILE INPUT DATA REGIONS  
RECS= 21 INPUT

THE BOSTONIAN • APRIL 1865.